Article

Immunity

Most Tissue-Resident Macrophages Except Microglia Are Derived from Fetal Hematopoietic Stem Cells

Graphical Abstract

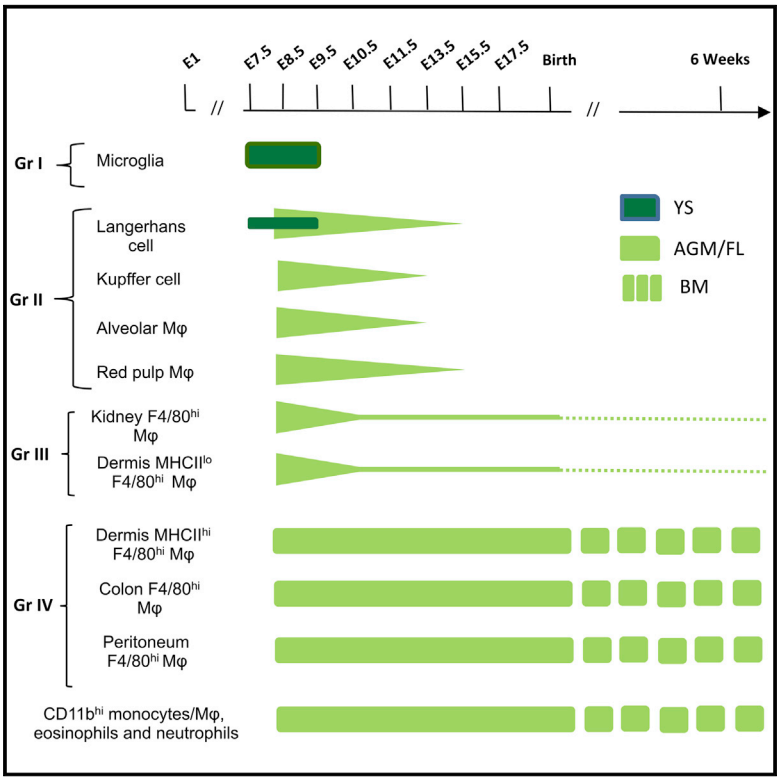

Highlights

- *Kit*^{MercreMer} fate mapping mouse strain for hematopoietic system was developed
- Most tissue resident macrophages are derived from hematopoietic stem cells
- Microglia represent the only tissue derived wholly from yolk sac precursors
- Four groups of tissue macrophages can be defined by their recruitment kinetics

Authors

Jianpeng Sheng, Christiane Ruedl, Klaus Karjalainen

Correspondence

ruedl@ntu.edu.sg (C.R.), klaus@ntu.edu.sg (K.K.)

In Brief

Most resident macrophages originate from fetal sources and then self-renew in situ to maintain their numbers through the lifetime of the mouse. Karjalainen and colleagues show here that most resident macrophages, brain microglia excluded, are descendants of fetal hematopoietic stem cells and not from yolk sac precursors as suggested previously.

Sheng et al., 2015, Immunity *43*, 382–393
August 18, 2015 ©2015 Elsevier Inc.
http://dx.doi.org/10.1016/j.immuni.2015.07.016

CellPress

CellPress

Immunity
Article

Most Tissue-Resident Macrophages Except Microglia Are Derived from Fetal Hematopoietic Stem Cells

Jianpeng Sheng,[1] Christiane Ruedl,[1,*] and Klaus Karjalainen[1,*]
[1]School of Biological Sciences, Nanyang Technological University, 60 Nanyang Drive, Singapore 637551, Singapore
*Correspondence: ruedl@ntu.edu.sg (C.R.), klaus@ntu.edu.sg (K.K.)
http://dx.doi.org/10.1016/j.immuni.2015.07.016

SUMMARY

Macrophages are one of the most diverse cell populations in terms of their anatomical location and functional specialization during both homeostasis and disease. Although it has been shown in different fate mapping models that some macrophages present in adult tissues are already established during fetal development, their exact origins are still under debate. In the current study, we developed a fate mapping strain, based on the *Kit* locus, which allowed us to readdress "the origins" question. Different types of macrophages from various adult tissues were traced to their fetal or adult sources by inducing labeling in precursors at several time points either during fetal development or in adult mice. We show that all adult macrophages, resident or infiltrating, are progenies of classical hematopoietic stem cells (HSC) with the exception of microglia and, partially epidermal Langerhans cells, which are yolk sac (YS)-derived.

INTRODUCTION

Ilya Mechnikov was the first to describe macrophages in the late 19th century as large phagocytic cells (macro "big" + phage "eat"). Although these features are common to all macrophages, these cells exhibit high plasticity in terms of their functional diversity. They have important roles in organ development, tissue homeostasis and repair, in addition to their roles as effectors of innate immunity (Wynn et al., 2013). Macrophages are traditionally defined and categorized by their anatomical territory. Examples include brain microglia, liver Kupffer cells and lung alveolar, splenic red pulp, and peritoneal macrophages.

The established concept of the mononuclear phagocytic system (MPS) has been used to unify such a diverse cell type as one functional entity. According to this concept, monocytes developing in the bone marrow (BM) continuously colonize different tissues and mature into macrophages in situ. However, this concept has been challenged recently and thought to be an oversimplification. The first evidence that tissue macrophages can develop from embryonic sources and bypass monocytic intermediates came from microglia-resident macrophages in brain parenchyma. Based on the *Runx1*^{MercreMer} fate mapping mouse, microglia were shown to be derived from embryonic day 7.5 (E7.5) yolk sac (YS) precursors (Ginhoux et al., 2010). Furthermore, based on *Csf1r*^{MercreMer} fate mapping mouse, YS origin was generalized to many macrophages in other tissues including epidermis, liver, spleen, lung, pancreas, and kidney (Schulz et al., 2012). In a study from Schulz et al., the authors noted that tissue macrophages can consist of different pools of cells based on F4/80 and CD11b expression: F4/80^{hi} macrophages were postulated to be derived from YS precursors that were able to maintain their numbers in situ (resident), while CD11b^{hi} macrophages were thought to be replaced continuously by BM-generated monocytes (infiltrating) (Schulz et al., 2012). In a subsequent study, F4/80^{hi} resident macrophages were proposed to originate from YS-derived erythro-myeloid progenitors (EMPs) (Gomez Perdiguero et al., 2015).

Although the prenatal origin and local maintenance of F4/80^{hi} tissue macrophages were confirmed by other studies (Hashimoto et al., 2013; Yona et al., 2013), conflicting reports have also been put forward suggesting a different origin for F4/80^{hi} tissue macrophages. For example, Langerhans cells (LCs) were reported to originate from YS precursors by Schulz et al. (2012), whereas Hoeffel et al. (2012) reported that they originated predominately from fetal liver (FL) monocytes. Similarly, lung alveolar macrophages were shown to originate from YS progenitors by Schulz et al. (2012), but two other studies found that they originated from fetal monocytes via a granulocyte macrophage colony stimulating factor (GM-CSF)-dependent pathway (Guilliams et al., 2013; Schneider et al., 2014) with minimal contribution from BM (Hashimoto et al., 2013).

Although microglia are commonly accepted to be derived from YS precursors (Epelman et al., 2014; Ginhoux et al., 2010; Kierdorf et al., 2013; Gomez Perdiguero et al., 2015; Schulz et al., 2012), the nature of these precursors has been debated. In one fate mapping study using *Runx1*^{MercreMer} mice, YS microglia precursors were already labeled at embryonic day 7–7.25 (E7–7.25) (Ginhoux et al., 2010), while in the *Csf1r*^{MercreMer} fate mapping model, precursors were only labeled starting at E8.5 and were suggested to represent EMPs (Bertrand et al., 2005b; Kierdorf et al., 2013; Gomez Perdiguero et al., 2015). Thus the origins of tissue macrophages remain unclear.

There are several limitations to the inducible fate mapping models currently available to study ontogenesis of tissue macrophages, including the *Runx1*^{MercreMer}, *Csf1r*^{MercreMer}, and *Cx3cr1*^{creER} mouse models (Ginhoux et al., 2010; Kierdorf et al., 2013; Gomez Perdiguero et al., 2015; Yona et al.,

CrossMark

2013). *Runx1* expression is required for the very early event of endothelial to hematopoietic cell transition, but not thereafter (Chen et al., 2009). Thus, *Runx1* expression is transient during early embryonic development and cannot be used to "tag" late precursors (Lacaud et al., 2002). *Csf1r*- and *Cx3cr1*-inducible fate mapping models also target macrophage progenitors and mature macrophages, complicating the interpretation of results.

Because Kit (CD117) is expressed in early YS and FL progenitors as well as in fetal and adult HSCs and their early progenies, but not in mature hematopoietic cells (Ivanova et al., 2002), we have generated a *Kit*^{MercreMer} mouse strain that allowed us to fate map with a different approach, adult macrophages and myeloid cells in various tissues at different time points of ontogeny. We show that all adult macrophages, resident and infiltrating, are derived from definitive hematopoiesis like neutrophils and lymphocytes. Exceptions include brain microglia and partially also epidermal Langerhans cells (LCs) that are descendants from YS precursors.

RESULTS

Generation of *Kit*^{MercreMer} Mouse and Strategy for Fate Mapping

In order to fate map the descendants of hematopoietic precursors from early embryonic, fetal, or adult stages, we generated a mouse strain containing an inducible *MercreMer* construct inserted into the 3′-UTR of the *Kit* gene, hereafter called *Kit*^{MercreMer} (Figure S1A). This insertion did not affect the expression of CD117 in BM cells (data not shown) and the crosses between *Kit*^{MercreMer} (BALB/c) and *Rosa26-loxP-STOP-loxP-eYFP* (C57BL/6) strains (*Kit*^{MercreMer}*R26*) could then be used as adults or as timed pregnancies for fate mapping. We gave single tamoxifen injections at different time points during gestation (E7.5, E8.5, E9.5, E11.5, E13.5, E15.5, or E17.5) or multiple injections during a 1-month period in adult mice to induce YFP labeling, which was then scored in different myeloid cells in embryos or in adult mice (Figure S1B). Importantly, short-lived peripheral blood neutrophils, T cells, and B cells were used as convenient internal control populations that reflect the activity of HSC and their primitive progenies. To increase rigor of analysis, we took comparative results of different tissues at a given time point from the same mouse as the peripheral blood neutrophils and lymphocyte controls.

Most Tissues Contain Three Phenotypically Similar Pools of Myeloid Cells

To identify target cells for fate mapping, we analyzed CD45$^+$ cells for CD11b and F4/80 expression using colonic lamina propria cells as a guide. Three major populations could be observed: F4/80^{hi} CD11b^{hi} (Fr I), F4/80^{int} CD11b^{hi} (Fr II), and F4/80^{lo} CD11b^{hi} (Fr III) cells (Figure 1). To further characterize the fractions, we analyzed them for macrophage markers defined by the recent Immunological Genome (ImmGen) Project (Gautier et al., 2012), including CD64, CD16/32, MerTK, and transgenic *Cx3cr1*$^{GFP/+}$ expression (core macrophage signatures). Using these criteria, the cells in Fr I belonged to macrophages corresponding to the so-called F4/80^{hi} resident cells (Schulz et al., 2012). In addition, these macrophages were CD11c$^+$ MHC II$^+$ and typically represented a homogenous population (Figure 1).

Fr II cells were further characterized based on Ly6C and MHC II expression (Tamoutounour et al., 2012; Jakubzick et al., 2013). At least four different cell subpopulations were delineated: Ly6C^{hi} MHC II$^{lo\ to\ hi}$ (IIa), Ly6C^{int} MHC II^{hi} (IIb), Ly6C^{lo} MHC II^{hi} (IIc), and Ly6C^{lo} MHC II^{lo} (IId). The phenotypes of cells in the IIa, IIb, and IIc sub-fractions suggested them to be monocytic and macrophage lineage cells with increasing maturity from IIa to IIc. A similar maturation cascade has also been observed in recent reports (Bain et al., 2014; Tamoutounour et al., 2013). The most abundant sub-fraction in the colon, IId, consisted of eosinophils as shown by Siglec-F and CCR3 expression but very low CD117 expression (Figure 1). Fr III (F4/80^{lo} CD11b^{hi}) cells appeared to represent typical neutrophils, as suggested by their Ly6G^{hi} Ly6C^{int} phenotype (Figure 1).

The same three major fractions found in the colon could be identified in most tissues examined (Table S1A), including the brain, colon, peritoneum, liver, kidney, spleen, lung, and dermis, although the relative expression of CD11b and F4/80 varied in different tissues (Figure 2). For example, Fr I F4/80^{hi} CD11b^{lo} cells in the lung appeared to be alveolar macrophages as they were the major cell type in bronchoalveolar lavage (BAL) fluid, while Fr I macrophages in the peritoneum were F4/80^{hi} CD11b^{hi} (Figure 2). The epidermis almost entirely consisted of macrophages (Fr I, LCs) with hardly any detectable Fr II (monocytes, macrophages, and eosinophils) or Fr III (neutrophils) (Figure 2). Classically-defined tissue resident macrophages such as Kupffer cells, alveolar macrophages, and spleen red pulp macrophages belonged to Fr I (F4/80^{hi}), thus "Fr I phenotype cells" in other organs most likely represent resident macrophages (Hashimoto et al., 2013).

Fr I resident macrophages typically represented a homogenous population as revealed by CD11c and MHC II staining. However, an exception to this was noted in Fr I cells of the dermis where two separate MHC II^{lo} and MHC II^{hi} macrophage populations were observed (Figure 2). Similar populations have been reported in an independent study based on CCR2 and CD64 staining (Tamoutounour et al., 2013).

The relative representation of sub-fractions (monocytes, macrophages, and eosinophils) in the Fr II population varied between different tissues. For example, the colon had a dominant eosinophil population, whereas the kidney had a dominant monocyte subpopulation (Figure 2). The peritoneal Fr II population consisted mainly of mature macrophages (Fr II c). It is very likely that peritoneal MHC II^{lo} Fr I (F4/80^{hi}) cells represented *Gata6*-dependent macrophages while MHC II^{hi} Fr II cells represented *Gata6*-independent macrophages (Okabe and Medzhitov, 2014; Rosas et al., 2014), originally described by Ghosn et al. (2010).

Neutrophils (Fr III) typically represented a minor population in tissues with the exception of the brain and lung where steady-state neutrophils were abundant, probably representing large marginated pools (Hogg and Doerschuk, 1995; Summers et al., 2010). Of note, brain Fr I cells (microglia) were CD45^{int} and could therefore be separated from CD45^{hi} Fr II and III cells that represented perivascular populations (Aloisi et al., 2000). Further characterization of perivascular Fr III cells clearly showed them to be classical neutrophils (Figure S2).

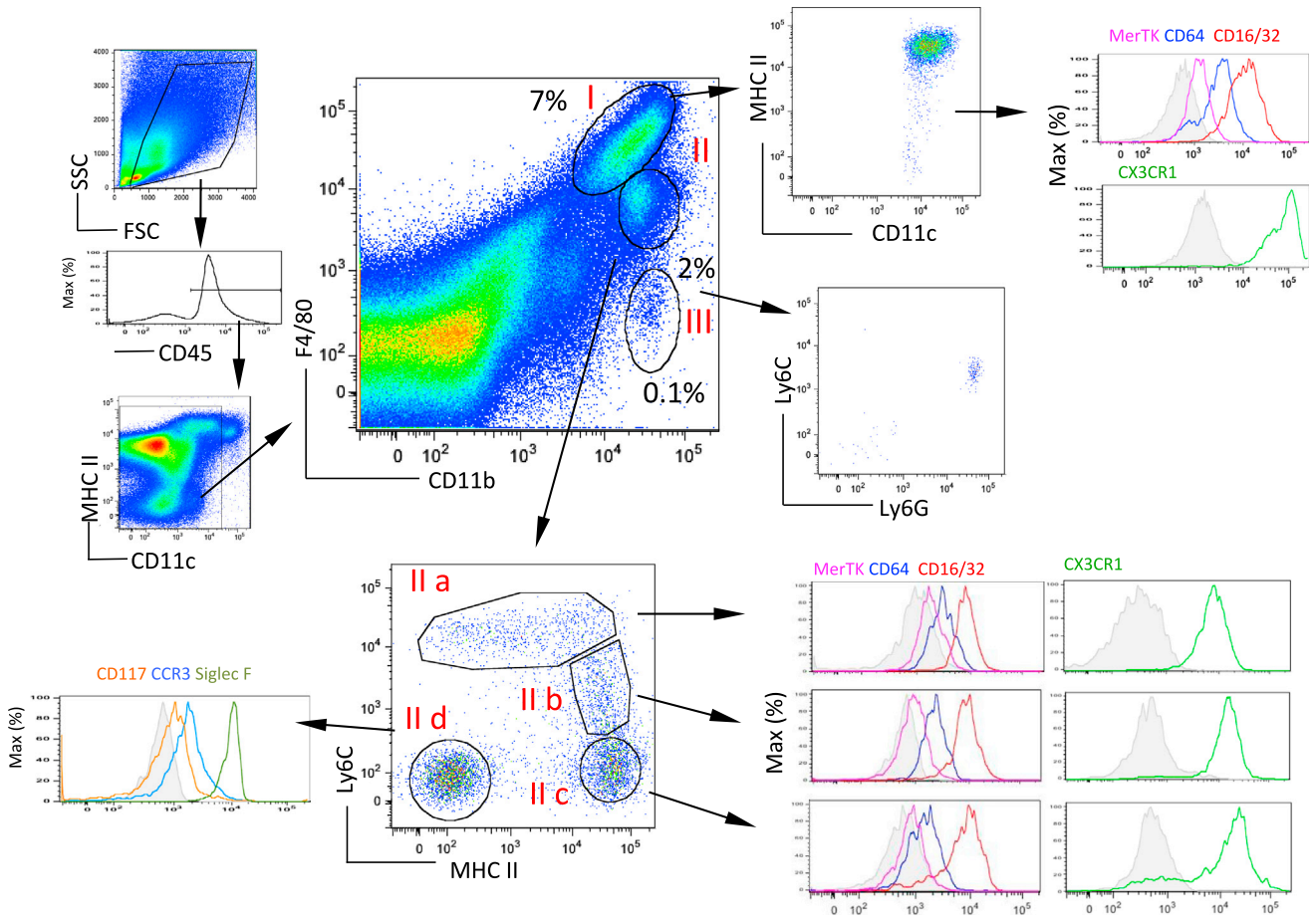

Figure 1. Characterization of Myeloid Cell Subsets as Targets for Fate Mapping

Gating and staining strategy exemplified with colon lamina propria cells: After gating out CD11c^{hi} MHC II^{hi} DCs, CD45^{+} cells comprised three major myeloid cell fractions: F4/80^{hi} CD11b^{hi} cells (Fr I), F4/80^{int} CD11b^{hi} (Fr II), and F4/80^{lo} CD11b^{hi} (Fr III). Fr I cells were MHC II^{+} CD11c^{+} and positive for several core macrophage signature markers, including CD64, CD16/32, MerTK, and CX_3CR1. Ly6C and MHC II staining divided the Fr II cells into at least four sub-fractions. Ly6C^{-} MHC II^{-} cells (Fr II d) are classical eosinophils (Siglec-F^{+} CCR3^{+} CD117^{-}). Ly6C^{hi} MHC II$^{-\text{ to }hi}$ cells (Fr II a) are monocytes. Ly6C^{-} MHC II^{hi} cells (Fr II c) are typical macrophages; i.e., positive for macrophage signature markers tested except MerTK. Fr II b cells were positive for macrophage signature markers but had intermediate expression of Ly6C and CX_3CR1. Fr III cells were typical Ly6G^{hi} Ly6C^{int} neutrophils. Data are representative of ten mice.

CD11b^{hi} Infiltrating Cells Are Derived from BM, while F4/80^{hi} Resident Macrophages Have Pre- or Post-Natal Origins

Because peripheral blood neutrophils are short-lived and constantly replaced by HSC-dependent BM progenitors, we used the labeling efficiency of peripheral blood neutrophils as a reference in our fate mapping experiments where label was induced in adult cells of *Kit*^{MercreMer}*R26* mice (Figure S1B). In the colon, neutrophils (Fr III) labeled to a similar degree as peripheral blood neutrophils, as was the case for all sub-fractions of CD11b^{hi} cells (Fr II), indicating that these cells were generated from adult BM progenitors (Figure 3A and Figure S3). Similar results were obtained with the same fractions from all the tissues examined (Table S1B). The percentage of DC labeling was also similar to that of peripheral blood neutrophils (Figure S4).

The labeling index of adult F4/80^{hi} tissue-resident macrophages (Fr I) differed by tissue (Figures 3A and 3C). Brain microglia, liver Kupffer cells, epidermal Langerhans cells, lung alveolar macrophages, and spleen red pulp macrophages were no longer labeled when tamoxifen was administered at the adult stage, while kidney and dermis MHC II^{lo} macrophages were only labeled to a small degree. The above results suggested that these macrophage populations were derived from earlier precursors that could not be "tagged" in adult mice. Colon, peritoneum, and dermis MHC II^{hi} F4/80^{hi} Fr I macrophages were labeled after the adult injection regimen to a similar amount as peripheral blood neutrophils (Figures 3A and 3C), indicating their BM origin. Because the absolute labeling percentage in peripheral blood neutrophils varied in individual mice, but the relative labeling of peripheral blood neutrophils to other cell populations was constant regardless of the absolute labeling of peripheral blood neutrophils (Figure S3), we normalized the labeling intensities to that of peripheral blood neutrophils to minimize the unavoidable variation in absolute marking after tamoxifen injections between mice (Figures 3B and 3D).

Our results confirmed previous reports that intestinal and dermal MHC II^{hi} F4/80^{hi} macrophages originate from BM

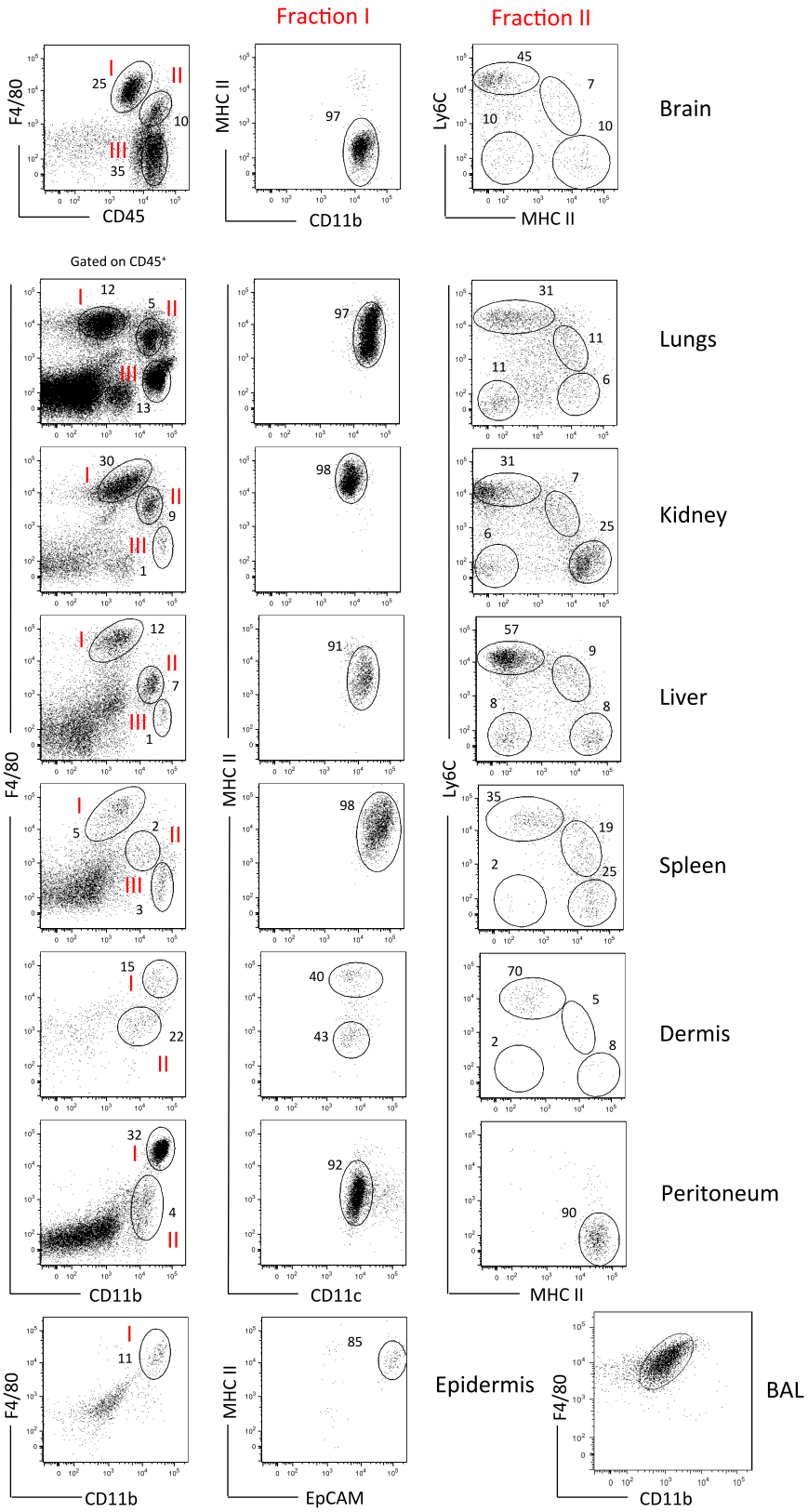

Figure 2. Three Common Cell Fractions Can Be Found in Most Tissues

The identification of three major cell fractions (Fr I, II, and III) in brain, lung, liver, kidney, spleen, peritoneum, and skin (dermis and epidermis) according to the strategy adopted in Figure 1 is shown. Brain myeloid cells were first gated in CD45^{int} cells, corresponding to microglia cells, and CD45^{hi} perivascular cells (upper panel). Epidermal Langerhans cells were defined as Fr I cells that were strongly positive for EpCAM and MHC II. Data are representative of ten mice. See also Figure S2.

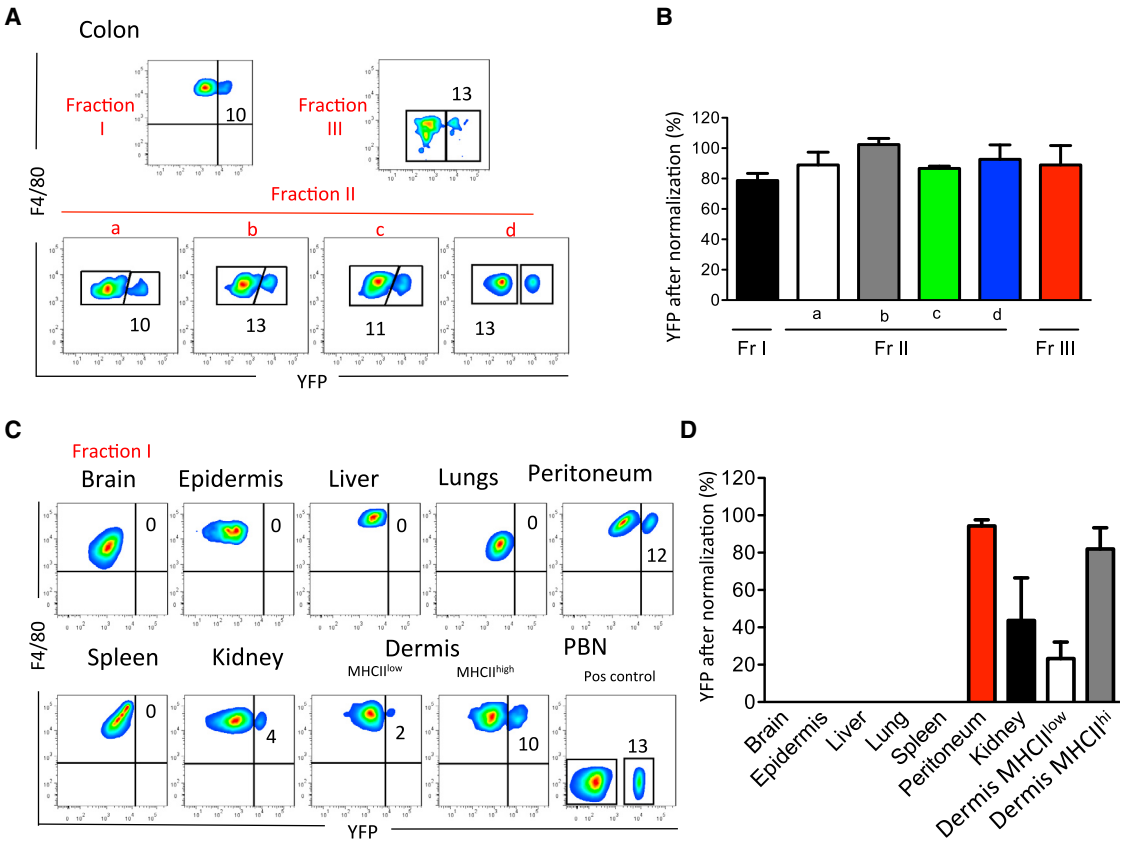

Figure 3. Fate Mapping of Adult BM Progenitors Predicts the Presence of Different Precursor Sources for Myeloid Cells

Adult fate mapping was performed as per Figure S1B and gating as per Figures 1 and 2. Peripheral blood neutrophils acted as internal controls for labeling efficiency, and the tracings shown are from the same mouse for (A) and (C).

(A) Colon myeloid cells as examples. Fr I macrophages, all Fr II subpopulations (F4/80^{int} CD11b^{hi}, infiltrating cells) and tissue neutrophils were labeled to the same degree as peripheral blood neutrophils. Data are representative of eight mice. See also Figure S3.

(B) Labeling efficiency of colon myeloid cells was normalized to peripheral blood neutrophils. Data represent means ± SEM of eight mice.

(C) Labeling of tissue-resident macrophages. Brain microglia, epidermal LCs, Kupffer cells, lung alveolar macrophages, and spleen red pulp macrophages were not labeled. Kidney and MHC II^{lo} dermal resident macrophages were partially labeled. Resident macrophages in the colon, peritoneum, and MHC II^{hi} dermal resident macrophages were labeled to the same degree as peripheral blood neutrophils. Data are representative of eight mice.

(D) Labeling efficiency of tissue-resident macrophages (Fr I) in other tissues was normalized to peripheral blood neutrophils. Data represent means ± SEM of eight mice. See also Figures S1 and S3–S6.

monocytes (Bain et al., 2014; Rivollier et al., 2012; Tamoutounour et al., 2013; Zigmond and Jung, 2013). However, as discussed below, our observations regarding the turnover of adult peritoneal macrophages disagree with previous studies that suggest they form a local, autonomously maintained population (Hashimoto et al., 2013; Yona et al., 2013). We did not observe any neutrophilia in the peritoneum (Figure S5), which excludes inflammation as a cause for macrophage turnover. In addition, peritoneal B1 cells were hardly tagged by adult tamoxifen treatment as would be expected (Figure S5). To further substantiate the importance of a continuous supply of BM to peritoneal macrophages, we gave a single large tamoxifen pulse at the adult stage and monitored the appearance of the labeled cells in BM, blood, and peritoneum. Labeled peritoneal macrophages were first detected at day 5 preceded by the appearance of the label in BM and blood neutrophils, strongly suggesting that peritoneal resident macrophages are derived from adult BM monocytes (Figure S6).

Peripheral blood T and B cells contained a lower percentage of label than peripheral blood neutrophils, reflecting the long half-lives of T and B cells. Large cohorts of unlabeled T and B cells were able to develop prior to the first adult tamoxifen injection (first injection at 6 weeks) thereby diluting the labeling percentage of newly generated blood lymphocytes (Figure S3).

Early YS Precursors Contribute to Adult Microglia and Langerhans Cells

Because many lineages of tissue-resident macrophages cannot be traced into adult BM progenitors, their precursors must have been present during earlier stages of hematopoiesis. Early YS precursors can be tagged in the *Runx1*^{MercreMer} system (Ginhoux et al., 2010). Therefore, we wanted to test whether these early YS precursors can also be labeled in our system in order to study their contribution to resident macrophage populations. To do this, we gave a single injection of tamoxifen at E7.5 to label *Kit*^{MercreMer}R26 embryos and measured the percentage of

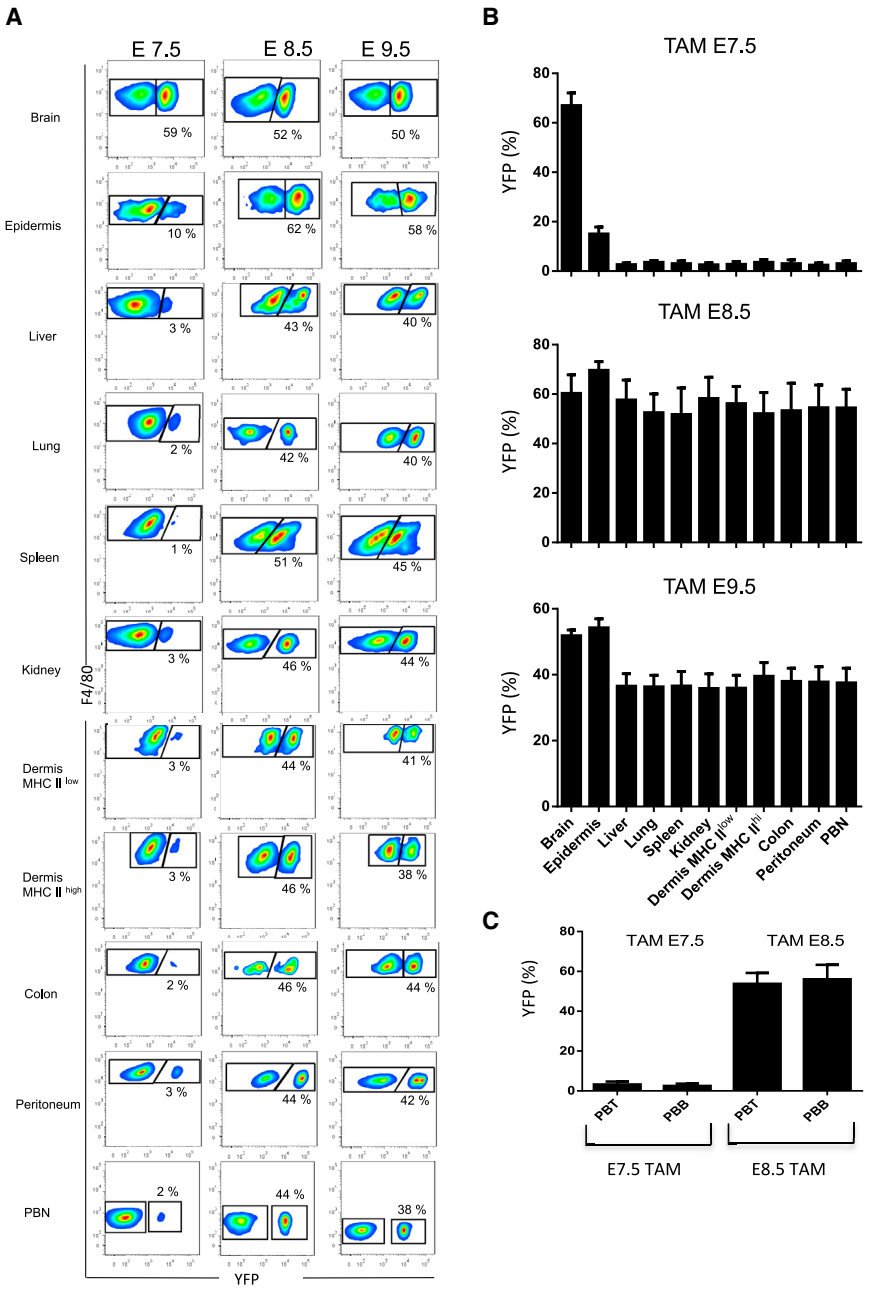

Figure 4. Fate Mapping of Embryonic Precursors Identify Adult Progenies from Two Hematopoietic Waves

(A) A single injection of tamoxifen was given at E7.5, E8.5, or E9.5 (Figure S1B) to label *Kit*^{MercreMer}*R26* embryos and the percentage of labeled tissue-resident Fr I cells was measured at 6 weeks of age for microglia, epidermal LCs, liver Kupffer cells, lung alveolar cells, spleen red pulp macrophages, and resident macrophages of the kidney, dermis, colon, and peritoneum. Peripheral blood neutrophils were used as internal controls. Gating was performed as shown in Figures 1 and 2. The tracings shown are from the same mouse at the indicated time point of tamoxifen injection.

(B) Bars represent means ± SEM of four to seven mice for each time point.

(C) YFP labeling efficiency of peripheral blood T and B cells are shown. Data represent means ± SEM of four to seven mice for each time point. See also Figure S1.

Most Adult Resident Macrophages Are Derived from a Second Wave of Hematopoiesis Driven by Classical HSCs

Definitive (HSC-producing) hematopoiesis starts at approximately E8.5 at the para-aortic splanchnopleura (PSp) that develops in the aorta-gonad-mesonephros (AGM). From here, cohorts of HSCs later (at E10.5) colonize the fetal liver (FL) where they undergo expansion and early differentiation (Cumano and Godin, 2007). To capture this and ongoing YS waves, we injected a single dose of tamoxifen at E8.5 or E9.5 to induce YFP label in *Kit*^{MercreMer}R26 embryos and again scored the percentage of labeling in resident macrophages, control peripheral blood neutrophils, and lymphocytes in 6-week-old adult mice (Figure S1B).

We could induce the label in adult microglia as efficiently at E8.5 or E9.5 (~50%) as at E7.5. Because blood circulation is established around E9.5, which is essential for microglia seeding (Ginhoux et al., 2010), the same population of YS precursors was labeled over the 3 day period and therefore no dilution of microglia label by later precursors was detected (and see below). These findings are consistent with the combined results of previous studies using either *Runx1*^{MercreMer} or *Csf1r*^{MercreMer} fate mapping mice (Ginhoux et al., 2010; Kierdorf et al., 2013; Gomez Perdiguero et al., 2015; Schulz et al., 2012).

Unlike adult microglia, which displayed similar percentages of labeling after injection of tamoxifen at E7.5, 8.5, or 9.5, all other resident macrophages and control peripheral blood neutrophils and lymphocytes showed dramatically different labeling kinetics and could not be labeled with a tamoxifen pulse at E7.5.

labeling in different resident macrophage populations in 6-week-old adult mice (Figure S1B).

Consistent with earlier studies with the *Runx1*^{MercreMer} mouse (Ginhoux et al., 2010), we could label adult microglia with high efficiency (>50%). All other tissue-resident macrophages including alveolar, kidney, spleen red pulp, dermal, and Kupffer cell populations labeled very poorly, similarly as control peripheral blood neutrophils and T and B cells (1%–3%). The only exception were LCs, which showed clear labeling (~10%), suggesting that later waves of precursors had diluted the original "~50% labeled population" (cf. microglia) (Figure 4). These results are in good agreement with a previous report (Hoeffel et al., 2012), showing that LCs are only partially derived from YS precursors.

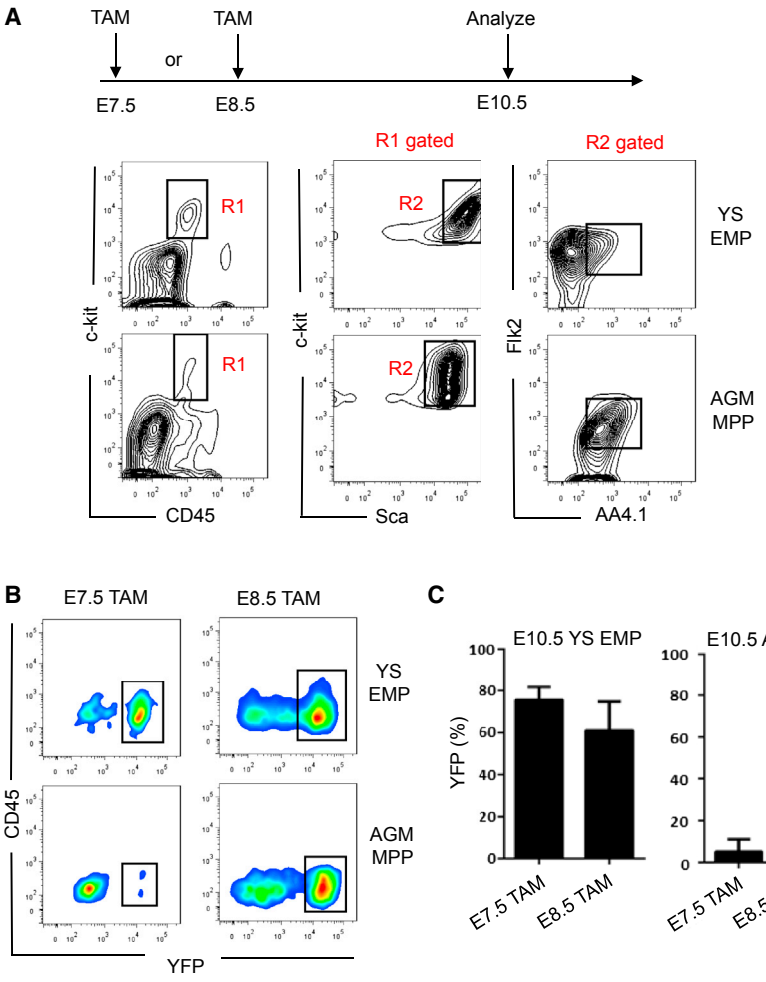

Figure 5. Early Embryonic Fate Mapping Labels YS EMPs and AGM Precursors with Different Kinetics

After a single pulse of tamoxifen at E7.5 or E8.5 to label *Kit*^{MercreMer}*R26* embryos, YS and AGM were analyzed at E10.5.

(A) YS EMPs and AGM MPPs were first gated on the kit$^+$ CD45^{lo} population, the majority of which was Sca-1$^+$. AA4.1 was used to further identify both populations.

(B and C) YFP$^+$ YS EMPs and AGM MPPs analyzed at E10.5 after E7.5 or E8.5 tamoxifen pulse. Representative plots are shown in (B), and data from (C) represent means ± SEM of six embryos in each group. See also Figure S1.

However, after an E8.5- or 9.5-pulse of tamoxifen, all non-microglial adult macrophages, together with peripheral blood neutrophils and lymphocyte controls, reached a similar robust labeling index (~40%).

We refer to this pattern as an HSC wave because the kinetics of labeling coincide with the appearance of HSCs and also, importantly, because many cell types (peripheral blood neutrophils, lymphocytes, and macrophages) representing the typical adult output of HSCs shared a similar labeling intensity. Notably, the labeling index of LCs (as mentioned above) increased from ~10% at E7.5 to ~60% at E8.5 or 9.5 (not to ~40% as seen for the other cells). This, indeed, suggests that LCs are descendants from two sources, HSC and YS waves.

Early Fetal Fate Mapping Reveals the Progenitors of YS and HSC Waves

In order to identify the potential progenitors responsible for YS and HSC waves, we induced tagging in *Kit*^{MercreMer}R26 embryos at E7.5 or E8.5 and scored the labeling index at E10.5 in YS and AGM progenitors (Figure 5). We used conventional markers to identify EMPs in YS and AGM multipotent progenitors (MPPs) as CD45^{lo} Kit^{hi} Sca-1$^+$AA4.1$^+$ cells (Figure 5A). Of note, the AA4.1$^+$ portion of Kit$^+$ Sca-1$^+$ cells were larger for AGMs, in good agreement with a previous study (Bertrand et al., 2005a). Induction at E7.5 lead to robust labeling of YS EMPs (~70%), similar to that induced by the E8.5 pulse (Figure 5B). Because we can robustly label YS EMPs with the E7.5 tamoxifen pulse, but not adult resident macrophages other than microglia, our results strongly suggest that EMPs are not the source of adult resident macrophages as proposed previously (Gomez Perdiguero et al., 2015).

AGM MPPs could not be labeled with the E7.5 pulse and were only labeled later at E8.5 (Figure 5B). This is consistent with the appearance of the first HSCs and their progenies in the AGM region at this time (Cumano and Godin, 2007). In addition, the E8.5 pulse is the earliest pulse that is able to induce strong labeling of adult resident macrophages, underlining the role of the HSC wave as their potential source.

Since YS and AGM precursors migrate to the FL to expand and further differentiate (Cumano and Godin, 2007; Palis et al., 1999), we wanted to see whether we could discriminate the descendants of YS and HSC waves in the FL by their labeling kinetics. To do this, label was induced in *Kit*^{MercreMer}R26 embryos at E7.5 or E8.5 and the amount of tagging was then scored at E13.5 or E16.5 in FL myeloid cells as defined earlier (Figure 6A).

In FL, we were able to identify neutrophils (Fr III, Ly6G$^+$), populations of monocytes (Fr IIa, Ly6C$^+$), and eosinophils (Fr IId, Ly6C$^-$Siglec-F$^+$), both of which were MHC II-negative, and resident macrophage-like cells (Fr I) (Figure 6A). Again, as in the case of the AGM fate mapped cells, we could not induce labeling with an E7.5 pulse in FL neutrophils (N), eosinophils (E), or monocytes (M), although YS EMPs were strongly tagged (Figures 5A and 6B). In fact, NEMs could only be labeled 1 day later at E8.5 (Figure 6B).

However, FL Fr I macrophages (probably direct migrants from YS) could be strongly tagged at E7.5 and these "early" labeled cells were diluted by latecomers into the FL (~45% E13.5 to ~10% E16.5), and even more so in adults (1%–3%) (Figures 6B and 3).

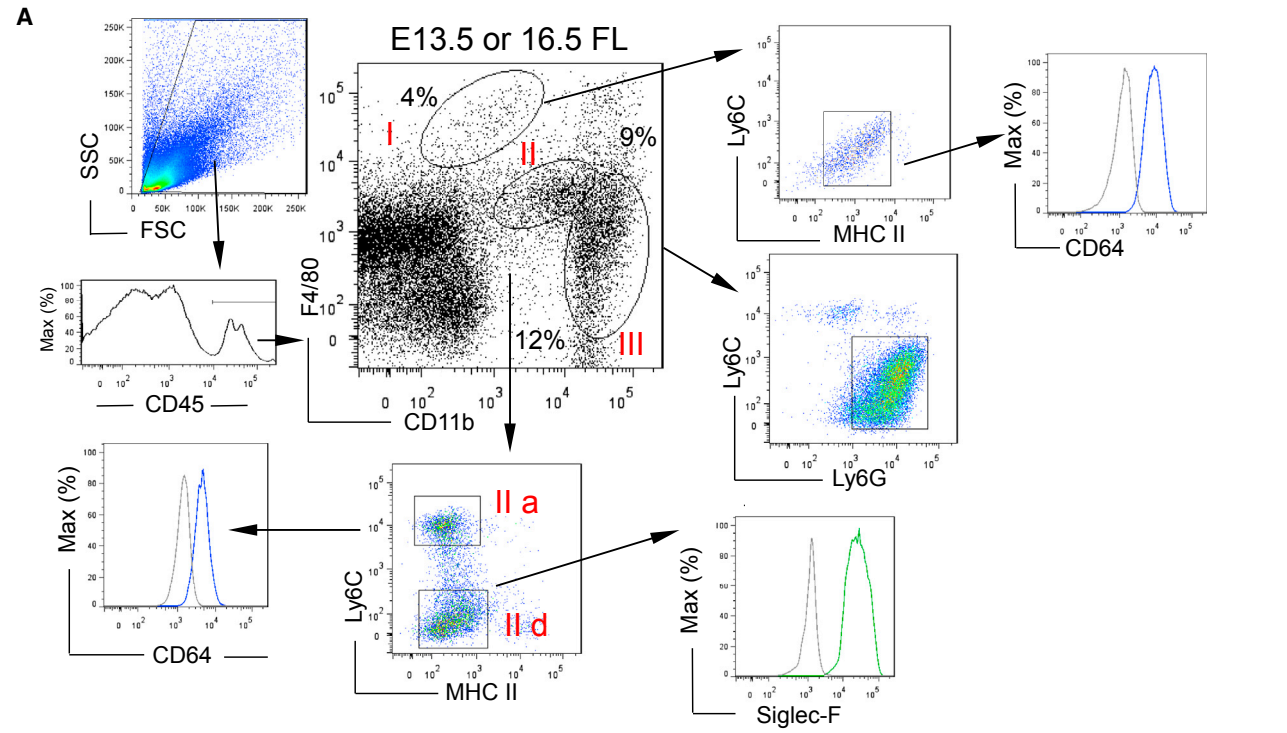

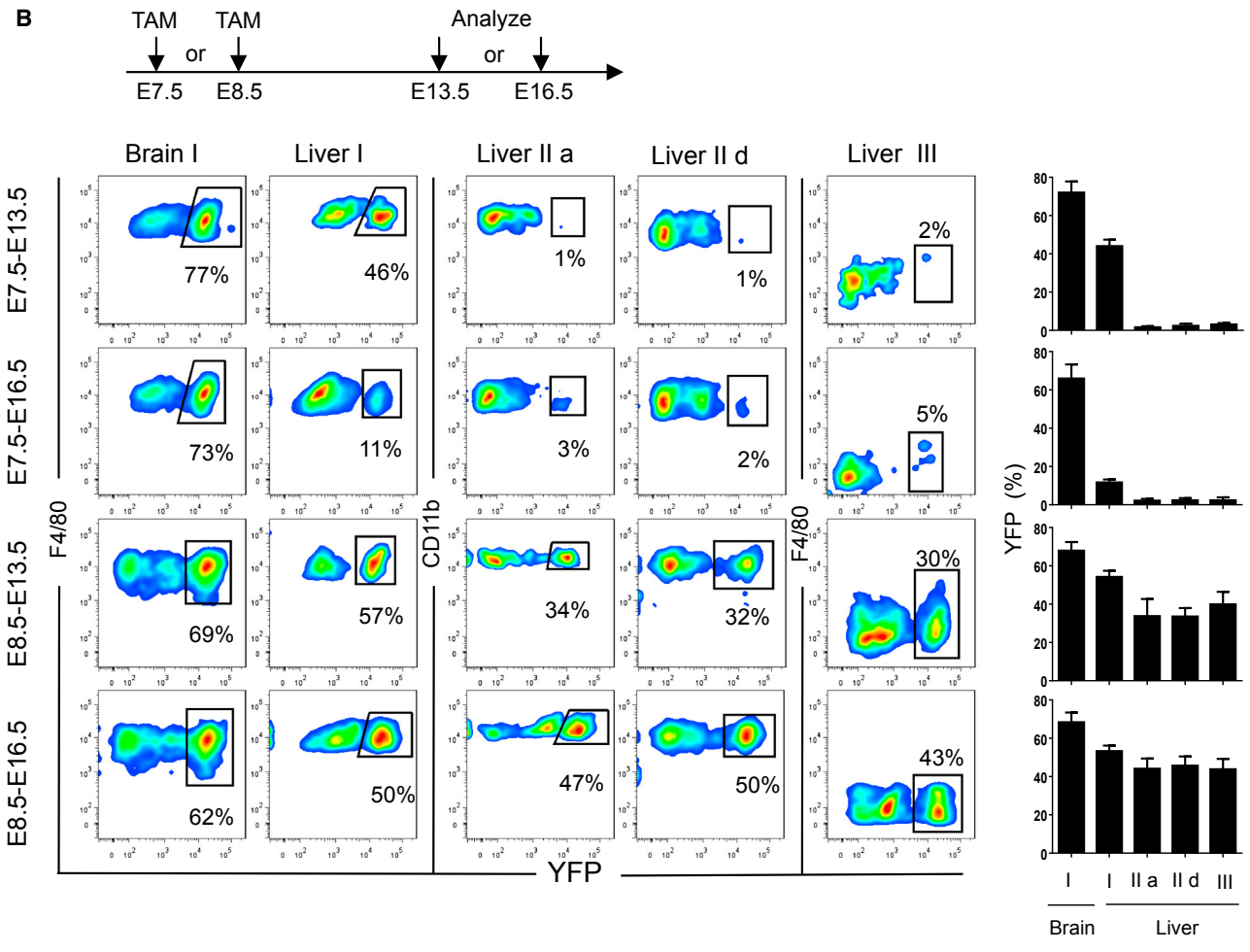

(legend on next page)

These FL tracing results support our conclusion that the HSC wave, originating from AGM, is the source of adult resident macrophages, and not YS EMPs, which contribute only to microglia and partially to LCs. In addition, FL monocytes that were first labeled at E8.5 could be the crucial intermediates for adult tissue resident macrophages and in fact, Hoeffel et al. showed very recently that FL monocytes can replace earlier YS-derived macrophages in most tissues (Hoeffel et al., 2015).

Different Tissue Resident Macrophages Show Characteristic Recruitment Windows

Because most adult tissues have stopped recruiting new resident macrophages (adult fate mapping), we wanted to study how long the new resident macrophages first initiated at E8.5 by the HSC wave continued to be recruited into tissues. To do this, we induced the YFP label in *Kit*^{MercreMer}R26 embryos at E11.5, 13.5, 15.5, or 17.5 when the FL has become the dominant source of hematopoiesis and then scored the labeling of resident macrophages in adult mice (Figure 1B). The amount of induced label in peripheral blood neutrophils was again used as a control because FL HSC or their primitive progenitors colonize the BM where they generate what will eventually become peripheral granulocytes and lymphocytes in adults.

Microglia, which are derived from early YS precursors, are not labeled at any of the above time points (Figure 7), which is consistent with previous reports that exclude a contribution from definitive hematopoiesis (Epelman et al., 2014; Ginhoux et al., 2010; Kierdorf et al., 2013; Gomez Perdiguero et al., 2015; Schulz et al., 2012). Most resident tissue macrophages were labeled to similar amount as peripheral blood neutrophils by the E11.5 pulse, however, when tamoxifen was injected at E13.5, 15.5, or 17.5, clear differences were detected in the labeling efficiency of F4/80^{hi} macrophages from different tissues (Figure 7A). Three trends could be observed (Figure 7B): Labeling percentage gradually decreased to zero in some tissue macrophages such as Kuppfer cells, LCs, alveolar macrophages, and spleen red pulp macrophages (Trend I). For kidney and dermis MHC II^{lo} F4/80^{hi} macrophages, labeling efficiency decreased but was then maintained at a lower level (Trend II). For colon, peritoneum, and dermis MHC II^{hi} F4/80^{hi} macrophages, labeling efficiency was similar to peripheral blood neutrophils across all time points (Trend III). Our results confirm the fetal origins of most resident macrophages. However, our findings strongly suggest the fetal hematopoietic stem cells and not the YS-derived precursors as a source for these cells.

DISCUSSION

In order to identify targets for our fate mapping experiments, we initially refined the characterization of myeloid cells in several different tissues. In almost all tissues analyzed (excluding the epidermis, dermis, and peritoneum), we can identify three major populations of myeloid cells (excluding DCs) based on CD11b and F4/80 expression, with some minor variations: F4/80^{hi} resident macrophages (Fr I), CD11b^{hi} infiltrating cell mixtures (Fr II), and neutrophils (Fr III). CD11b^{hi} cells consist of a mixture of monocytes, macrophages, and eosinophils. The composition of CD11b^{hi} cell mixtures varied slightly across different tissues e.g., the colon has a major eosinophil fraction, while the kidney has an abundant monocyte population.

Adult fate mapping showed that all infiltrating CD11b^{hi} cell mixtures (Fr II) and neutrophils (Fr III), in all tissues tested, became labeled to a similar extent as peripheral blood neutrophils, suggesting that adult BM HSC or primitive long-lived progenitors are the source of these cells. However, tissue-resident macrophages, i.e., F4/80^{hi} (Fr I) cells, namely brain microglia, liver Kuppfer cells, epidermal LCs, and spleen red pulp, lung alveolar, and most of the kidney, behaved differently, and dermal MHC II^{lo} macrophages could not be induced to carry label after adult tamoxifen pulses because their origins are from prenatal precursors (further discussed below). Colonic, dermal MHC II^{hi}, and peritoneal macrophages labeled in a similar manner to peripheral blood neutrophils, suggesting a high turnover and continuous supply from adult BM. These results confirmed previously reported observations that intestinal and dermal MHC II^{hi} F4/80^{hi} macrophages originate from BM monocytes (Bain et al., 2014; Rivollier et al., 2012; Tamoutounour et al., 2013; Zigmond and Jung, 2013). However, peritoneal macrophages were thought to represent a self-renewing, autonomous local pool (Hashimoto et al., 2013; Yona et al., 2013), which is in disagreement with our results. In the adult fate mapping study of Yona et al. using *Cx3cr1*^{creER} mice, peritoneal macrophages were not labeled, which is the opposite of what we would have expected because, according to our observations, their monocyte precursors were CX_3CR1-positive. In their study, only tissue macrophages that were themselves strongly CX_3CR1-positive were labeled in *Cx3cr1*^{creER} mice. However, the authors did not show whether they could label other monocyte-dependent CX_3CR1-negative macrophages (as positive controls), e.g., dermal MHC II^{hi} cells, in *Cx3cr1*^{creER} mice to validate the robustness of their approach under steady-state conditions (Yona et al., 2013). The authors also showed that under inflammatory conditions, monocytes were recruited into the peritoneum where they became MHC II^{hi} macrophages that later developed into MHC II^{lo} cells. However, under normal conditions, 1%–10% of peritoneal macrophages are in fact MHC II^{hi} (Okabe and Medzhitov, 2014; Rosas et al., 2014; Ghosn et al., 2010), so we could argue that steady-state MHC II^{lo} macrophages are also derived from infiltrating monocytes via transitional MHC II^{hi} macrophages. In addition, the parabiosis data of Hashimoto et al. speak clearly for self-renewing peritoneal macrophages although some of their fate mapping results could also support the idea of partial contribution from adult BM. The discrepancy between their and our findings could be explained by the differences in mouse strains C57BL/6 versus (BALB/c × C57BL/6) F1 or their housing conditions that can certainly have influence in this compartment.

Our major finding that all tissue-resident macrophages, except brain microglia and to some extent, epidermal LCs, are

Figure 6. Progenies of Two Hematopoietic Waves Can Be Detected in Fetal Liver

(A) The gating strategy for characterization of FL myeloid cells, which follows the conventions of Figure 2, is shown.

(B) After a single pulse of tamoxifen at E7.5 or E8.5, as indicated, microglia and fetal liver were analyzed at E13.5 and E16.5. Representative plots are shown on the left and the combined data on the right represent means ± SEM of three to six embryos in each group. See also Figure S1.

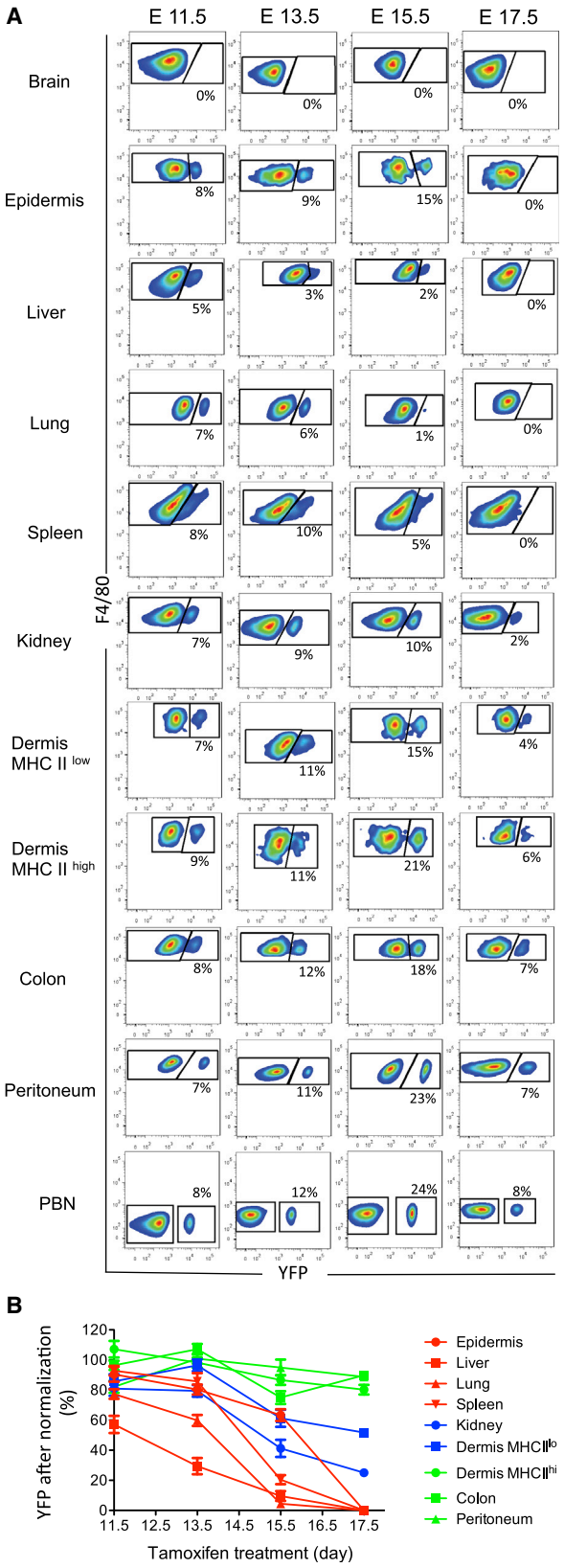

Figure 7. Characteristic Recruitment Windows for Different Tissues

Tamoxifen was given at E11.5, E13.5, E15.5, or E17.5 to label *Kit*^{MercreMer}*R26* embryos using the experimental scheme shown in Figure 4.

(A) Data are representative of five to ten mice for each time point. Plots corresponding to a given time point, were from the same mouse.

(B) Graphical representation of the normalized labeling efficiency (with peripheral blood neutrophils) of different tissues across different time points shows three major trends, indicated in different colors. Data represent means ± SEM with five to ten mice in each group. See also Figure S1.

generated by definitive intra-embryonic hematopoiesis challenges the view that most tissue-resident adult macrophages are derived from extra-embryonic YS precursors defined as EMPs (Gomez Perdiguero et al., 2015; Schulz et al., 2012). Our strongest evidence against the "EMP hypothesis" is that although we could strongly label YS EMPs (E10.5) by inducing tagging in *Kit*^{MercreMer}R26 embryos at E7.5, we were not able to detect any clear tagging in adult tissue-resident macrophages, except microglia and some LCs. Similarly, FL monocytes, neutrophils, or eosinophils (E13.5 and 16.5) remained unlabeled. Yet, a tamoxifen pulse, 1 day later at E8.5, labeled all adult non-microglial tissue-resident macrophages to the same extent as peripheral blood neutrophils and lymphocytes (apart from LCs which were labeled to a greater extent). In addition, the E8.5 pulse also labeled FL monocyte, neutrophil, and eosinophil populations efficiently. For simplicity, we refer to the emergence of labeled cells after the E8.5 pulse as an HSC wave because the timing corresponds to the beginning of definitive HSC-dependent hematopoietic activity in the AGM region of the embryo with a similar labeling index of many different cellular types (macrophages, neutrophils, and lymphocytes) reflecting the output of classical HSCs.

The main thrust of Gomez Perdiguero et al. that YS EMPs were the source of adult tissue-resident macrophages was the exploitation of *Csf1r*^{MercreMer} fate mapping mice (Gomez Perdiguero et al., 2015). A pulse of tamoxifen at E8.5 in these mice induced label at a later stage in YS and FL EMPs and also in FL hematopoietic progenies; however, due to low labeling frequency of adult tissue-resident macrophages, analysis of adult tissues was therefore considered uninformative. To exclude the contribution of definitive hematopoiesis as the source of adult tissue-resident macrophages, the authors used constitutively active *Flt3-cre* fate mapping mice because YS hematopoiesis, unlike definitive hematopoiesis, is not marked in this system. Although the *Flt3-cre* approach marks adult HSC progenies robustly, fetal HSC output is labeled relatively weakly, as also shown by Gomez Perdiguero et al. (2015). It is these same fetal HSCs and their progenies that became labeled in our system and which we claim to become a source of adult tissue-resident macrophages. Therefore, the absence of label in adult tissue-resident macrophages of *Flt3-cre* mice does not argue strongly against the contribution of fetal HSCs and their progenies. Our results are in good agreement with those obtained in their elegant *Tie2*^{MercreMer} fate mapping mice, the major difference being that even earlier precursors are tagged in the *Tie2*^{MercreMer} system.

Our staggered tamoxifen pulses at later time points during embryogenesis (E11.5, 13.5, 15.5, or 17.5) revealed individual recruitment windows for tissue-resident macrophages, during which the receiving tissues accepted newcomers, followed by

characteristic shut-off times for further recruitment. The microglia compartment was already closed at E11.5 and no labeled cells could be detected in adult microglia after the E11.5 pulse, consistent with previous studies (Ginhoux et al., 2010; Gomez Perdiguero et al., 2015). This also reflects our finding that the microglia is the only tissue that is solely derived from YS precursors under normal steady-state conditions. All other adult tissue-resident macrophages shared a similar robust labeling index with peripheral blood neutrophils and lymphocytes after the E11.5 pulse, i.e., they all share a source-definitive hematopoiesis. Differences in tissue recruitment characteristics started to appear with later embryonal pulses. Some tissues (as discussed above) did not shut off and continuously recruited new precursors (colon, peritoneal, and dermal MHC II^{hi} macrophages). Recruitment of tissue-resident macrophages of the kidney and the dermal MHC II^{lo} population occurred mainly during embryogenesis but continued at low level during the adult stage. The liver, lung, and spleen completely stopped recruiting new Kuppfer cells, alveolar macrophages, and red pulp macrophages, respectively, during embryogenesis (between E15.5–17.5) and from then on these tissues maintained their populations autonomously in steady-state conditions as observed for microglia.

Epidermal LCs are an exception as a result of their hybrid origins from YS and HSC waves. This raises the question of whether functional specializations exist between LCs of different origins, although current research seems to strongly suggest that the tissue niche is able to induce proper functional characteristics in the migrants regardless of their origins (Gentek et al., 2014; Lavin et al., 2014; Suzuki et al., 2014).

It would be particularly interesting to determine the functional consequences of an exchange of fully YS-derived microglia with one dominated by cells of adult monocyte origin, a situation that can arise after therapeutic or inflammatory perturbations.

EXPERIMENTAL PROCEDURES

Animals

Kit^{MercreMer} mice were generated in our laboratory. Briefly, a codon-optimized IRES-Mer-cre-Mer (Verrou et al., 1999) gene fusion was inserted into the 3′ untranslated region (20 bp after the stop codon) of the *Kit* gene in BALB/c embryonic stem cells (ESCs). Targeted ESCs were injected into C57BL/6 blastocysts and the chimeric mice generated were then backcrossed to BALB/c mice to transmit the *Kit*^{MercreMer} allele.

Cx3cr1-GFP and *Rosa26*$^{LSL\text{-}eYFP}$ transgenic mice were kindly provided by Florent Ginhoux (SIgN, A*Star, Singapore). *Kit*^{MercreMer} mice were mated with Rosa26$^{LSL\text{-}eYFP}$ generating (BALB/c × C57BL/6) F1 background mice that were then used in all experiments. Timing of embryonic development was estimated from the day of coitus, assuming vaginal plug formation as E0.5.

All transgenic mice were bred in the specific pathogen-free NTU animal facility. This study followed the National Advisory Committee for Laboratory Animal Research guidelines under the Animal & Birds (Care and Use of Animals for Scientific Purposes) Rules of Singapore. The protocol was approved by the by the Institutional Animal Care and Use Committee (IACUC) of the Nanyang Technological University of Singapore.

Isolation of Tissue Samples and Flow Cytometry

Blood samples were taken from the mice via the retro-orbital vein under anesthesia. BM cells were flushed out with PBS plus 2% fetal bovine serum. To obtain bronchoalveolar lavage (BAL), we injected 2 ml PBS and then retrieved through the trachea using a cannula.

For isolation of tissue macrophages, a protocol adapted from a previous study was followed (Purnama et al., 2014). Briefly, 10 mL of PBS were used to perfuse the mice after CO_2 euthanasia and tissues were dissected out and minced followed by 30–60 min incubation at 37°C with 100 μg/mL Collagenase (Roche Applied Science, Basel Switzerland,) and 20 Units/mL DNase I (Life Technologies). To prepare single cells, tissue suspensions were passed through a 19-gauge syringe. Leukocytes were enriched using a Percoll® gradient (GE Healthcare, Life Sciences). Single-cell suspensions were stained and then analyzed using a LSRII flow cytometer (Becton Dickinson). Data were analyzed with FlowJo software (TreeStar). The following antibodies were used: CD11c (clone: N418), CD19 (clone: 6D5), GR-1 (clone: RB6-8C5), CD11b (clone: M1/70), CD45 (clone: 30F11), Ly6C (HK1.4), Ly6G (clone: 1A8), EMR1 (also known as F4/80) (clone: BM8), CD64 (clone:X54-5/7.1), CD16/32 (clone:93), MHC II (clone: M5/114.15.2), CD117 (clone: 2B8), EpCAM (clone: G8.8), and CCR3 (clone: J073E5) all from BioLegend. Siglec-F (clone: E50-2400) was purchased from BD Biosciences. MerTK (clone: BAF591) was purchased from R&D Systems.

Induction of Cell Tagging with Tamoxifen and Isolation of Fetal Tissues

Tamoxifen (Sigma) was dissolved in corn oil (Sigma). Four mg per mouse of tamoxifen was administered by gavage for adult fate mapping or by intraperitoneal injection in pregnant mothers for embryo labeling. For a single tamoxifen pulse at adults, 16 mg was administered by gavage.

To harvest embryos at different time points, we euthanized pregnant female mice by carbon dioxide asphyxiation. Uterine horns were taken out from abdomen and embryos were harvested. Endometrial tissue and placenta around each embryo proper were removed under the microscope without puncturing YS. YS was then gently teased away from the embryo and FL was dissected out using forceps. To isolate AGM, upper and lower portions of the embryo were cut away from the embryo using fine needles. Extra tissue at dorsal and ventral was cut away without damaging the aorta. YS, FL, and AGM were then minced and digested the same way as adult tissues to get single cell suspensions.

Giemsa Staining

Giemsa staining solution (Sigma) was used according to the manufacturer's instructions.

SUPPLEMENTAL INFORMATION

Supplemental Information includes six figures and one tables and can be found with this article online at http://dx.doi.org/10.1016/j.immuni.2015.07.016.

AUTHOR CONTRIBUTIONS

K.K. conceived the study. J.S., C.R., and K.K. designed the experiments. J.S. performed experiments and analyzed the data. J.S., C.R., and K.K. wrote the manuscript.

ACKNOWLEDGMENTS

We thank Dr. Florent Ginhoux for CX_3CR1-GFP and *Rosa26*$^{LSL\text{-}eYFP}$ transgenic mice and discussions and Dr. Michael Reth for the *MercreMer* DNA construct. The authors would like also to thank Kerry McLaughlin of Insight Editing London for editing this manuscript. This work was supported by MOE Tier 1 RG49/13 to K.K.

Received: November 25, 2014
Revised: April 20, 2015
Accepted: June 1, 2015
Published: August 18, 2015

REFERENCES

Aloisi, F., Ria, F., and Adorini, L. (2000). Regulation of T-cell responses by CNS antigen-presenting cells: different roles for microglia and astrocytes. Immunol. Today *21*, 141–147.

Bain, C.C., Bravo-Blas, A., Scott, C.L., Gomez Perdiguero, E., Geissmann, F., Henri, S., Malissen, B., Osborne, L.C., Artis, D., and Mowat, A.M. (2014).

Constant replenishment from circulating monocytes maintains the macrophage pool in the intestine of adult mice. Nat. Immunol. *15*, 929–937.

Bertrand, J.Y., Giroux, S., Golub, R., Klaine, M., Jalil, A., Boucontet, L., Godin, I., and Cumano, A. (2005a). Characterization of purified intraembryonic hematopoietic stem cells as a tool to define their site of origin. Proc. Natl. Acad. Sci. USA *102*, 134–139.

Bertrand, J.Y., Jalil, A., Klaine, M., Jung, S., Cumano, A., and Godin, I. (2005b). Three pathways to mature macrophages in the early mouse yolk sac. Blood *106*, 3004–3011.

Chen, M.J., Yokomizo, T., Zeigler, B.M., Dzierzak, E., and Speck, N.A. (2009). Runx1 is required for the endothelial to haematopoietic cell transition but not thereafter. Nature *457*, 887–891.

Cumano, A., and Godin, I. (2007). Ontogeny of the hematopoietic system. Annu. Rev. Immunol. *25*, 745–785.

Epelman, S., Lavine, K.J., Beaudin, A.E., Sojka, D.K., Carrero, J.A., Calderon, B., Brija, T., Gautier, E.L., Ivanov, S., Satpathy, A.T., et al. (2014). Embryonic and adult-derived resident cardiac macrophages are maintained through distinct mechanisms at steady state and during inflammation. Immunity *40*, 91–104.

Gautier, E.L., Shay, T., Miller, J., Greter, M., Jakubzick, C., Ivanov, S., Helft, J., Chow, A., Elpek, K.G., Gordonov, S., et al.; Immunological Genome Consortium (2012). Gene-expression profiles and transcriptional regulatory pathways that underlie the identity and diversity of mouse tissue macrophages. Nat. Immunol. *13*, 1118–1128.

Gentek, R., Molawi, K., and Sieweke, M.H. (2014). Tissue macrophage identity and self-renewal. Immunol. Rev. *262*, 56–73.

Ghosn, E.E., Cassado, A.A., Govoni, G.R., Fukuhara, T., Yang, Y., Monack, D.M., Bortoluci, K.R., Almeida, S.R., Herzenberg, L.A., and Herzenberg, L.A. (2010). Two physically, functionally, and developmentally distinct peritoneal macrophage subsets. Proc. Natl. Acad. Sci. USA *107*, 2568–2573.

Ginhoux, F., Greter, M., Leboeuf, M., Nandi, S., See, P., Gokhan, S., Mehler, M.F., Conway, S.J., Ng, L.G., Stanley, E.R., et al. (2010). Fate mapping analysis reveals that adult microglia derive from primitive macrophages. Science *330*, 841–845.

Gomez Perdiguero, E., Klapproth, K., Schulz, C., Busch, K., Azzoni, E., Crozet, L., Garner, H., Trouillet, C., de Bruijn, M.F., Geissmann, F., and Rodewald, H.R. (2015). Tissue-resident macrophages originate from yolk-sac-derived erythro-myeloid progenitors. Nature *518*, 547–551.

Guilliams, M., De Kleer, I., Henri, S., Post, S., Vanhoutte, L., De Prijck, S., Deswarte, K., Malissen, B., Hammad, H., and Lambrecht, B.N. (2013). Alveolar macrophages develop from fetal monocytes that differentiate into long-lived cells in the first week of life via GM-CSF. J. Exp. Med. *210*, 1977–1992.

Hashimoto, D., Chow, A., Noizat, C., Teo, P., Beasley, M.B., Leboeuf, M., Becker, C.D., See, P., Price, J., Lucas, D., et al. (2013). Tissue-resident macrophages self-maintain locally throughout adult life with minimal contribution from circulating monocytes. Immunity *38*, 792–804.

Hoeffel, G., Wang, Y., Greter, M., See, P., Teo, P., Malleret, B., Leboeuf, M., Low, D., Oller, G., Almeida, F., et al. (2012). Adult Langerhans cells derive predominantly from embryonic fetal liver monocytes with a minor contribution of yolk sac-derived macrophages. J. Exp. Med. *209*, 1167–1181.

Hoeffel, G., Chen, J., Lavin, Y., Low, D., Almeida, F.F., See, P., Beaudin, A.E., Lum, J., Low, I., Forsberg, E.C., et al. (2015). C-Myb(+) erythro-myeloid progenitor-derived fetal monocytes give rise to adult tissue-resident macrophages. Immunity *42*, 665–678.

Hogg, J.C., and Doerschuk, C.M. (1995). Leukocyte traffic in the lung. Annu. Rev. Physiol. *57*, 97–114.

Ivanova, N.B., Dimos, J.T., Schaniel, C., Hackney, J.A., Moore, K.A., and Lemischka, I.R. (2002). A stem cell molecular signature. Science *298*, 601–604.

Jakubzick, C., Gautier, E.L., Gibbings, S.L., Sojka, D.K., Schlitzer, A., Johnson, T.E., Ivanov, S., Duan, Q., Bala, S., Condon, T., et al. (2013). Minimal differentiation of classical monocytes as they survey steady-state tissues and transport antigen to lymph nodes. Immunity *39*, 599–610.

Kierdorf, K., Erny, D., Goldmann, T., Sander, V., Schulz, C., Perdiguero, E.G., Wieghofer, P., Heinrich, A., Riemke, P., Hölscher, C., et al. (2013). Microglia emerge from erythromyeloid precursors via Pu.1- and Irf8-dependent pathways. Nat. Neurosci. *16*, 273–280.

Lacaud, G., Gore, L., Kennedy, M., Kouskoff, V., Kingsley, P., Hogan, C., Carlsson, L., Speck, N., Palis, J., and Keller, G. (2002). Runx1 is essential for hematopoietic commitment at the hemangioblast stage of development in vitro. Blood *100*, 458–466.

Lavin, Y., Winter, D., Blecher-Gonen, R., David, E., Keren-Shaul, H., Merad, M., Jung, S., and Amit, I. (2014). Tissue-resident macrophage enhancer landscapes are shaped by the local microenvironment. Cell *159*, 1312–1326.

Okabe, Y., and Medzhitov, R. (2014). Tissue-specific signals control reversible program of localization and functional polarization of macrophages. Cell *157*, 832–844.

Palis, J., Robertson, S., Kennedy, M., Wall, C., and Keller, G. (1999). Development of erythroid and myeloid progenitors in the yolk sac and embryo proper of the mouse. Development *126*, 5073–5084.

Purnama, C., Ng, S.L., Tetlak, P., Setiagani, Y.A., Kandasamy, M., Baalasubramanian, S., Karjalainen, K., and Ruedl, C. (2014). Transient ablation of alveolar macrophages leads to massive pathology of influenza infection without affecting cellular adaptive immunity. Eur. J. Immunol. *44*, 2003–2012.

Rivollier, A., He, J., Kole, A., Valatas, V., and Kelsall, B.L. (2012). Inflammation switches the differentiation program of Ly6Chi monocytes from antiinflammatory macrophages to inflammatory dendritic cells in the colon. J. Exp. Med. *209*, 139–155.

Rosas, M., Davies, L.C., Giles, P.J., Liao, C.T., Kharfan, B., Stone, T.C., O'Donnell, V.B., Fraser, D.J., Jones, S.A., and Taylor, P.R. (2014). The transcription factor Gata6 links tissue macrophage phenotype and proliferative renewal. Science *344*, 645–648.

Schneider, C., Nobs, S.P., Kurrer, M., Rehrauer, H., Thiele, C., and Kopf, M. (2014). Induction of the nuclear receptor PPAR-γ by the cytokine GM-CSF is critical for the differentiation of fetal monocytes into alveolar macrophages. Nat. Immunol. *15*, 1026–1037.

Schulz, C., Gomez Perdiguero, E., Chorro, L., Szabo-Rogers, H., Cagnard, N., Kierdorf, K., Prinz, M., Wu, B., Jacobsen, S.E., Pollard, J.W., et al. (2012). A lineage of myeloid cells independent of Myb and hematopoietic stem cells. Science *336*, 86–90.

Summers, C., Rankin, S.M., Condliffe, A.M., Singh, N., Peters, A.M., and Chilvers, E.R. (2010). Neutrophil kinetics in health and disease. Trends Immunol. *31*, 318–324.

Suzuki, T., Arumugam, P., Sakagami, T., Lachmann, N., Chalk, C., Sallese, A., Abe, S., Trapnell, C., Carey, B., Moritz, T., et al. (2014). Pulmonary macrophage transplantation therapy. Nature *514*, 450–454.

Tamoutounour, S., Henri, S., Lelouard, H., de Bovis, B., de Haar, C., van der Woude, C.J., Woltman, A.M., Reyal, Y., Bonnet, D., Sichien, D., et al. (2012). CD64 distinguishes macrophages from dendritic cells in the gut and reveals the Th1-inducing role of mesenteric lymph node macrophages during colitis. Eur. J. Immunol. *42*, 3150–3166.

Tamoutounour, S., Guilliams, M., Montanana Sanchis, F., Liu, H., Terhorst, D., Malosse, C., Pollet, E., Ardouin, L., Luche, H., Sanchez, C., et al. (2013). Origins and functional specialization of macrophages and of conventional and monocyte-derived dendritic cells in mouse skin. Immunity *39*, 925–938.

Verrou, C., Zhang, Y., Zürn, C., Schamel, W.W., and Reth, M. (1999). Comparison of the tamoxifen regulated chimeric Cre recombinases MerCreMer and CreMer. Biol. Chem. *380*, 1435–1438.

Wynn, T.A., Chawla, A., and Pollard, J.W. (2013). Macrophage biology in development, homeostasis and disease. Nature *496*, 445–455.

Yona, S., Kim, K.W., Wolf, Y., Mildner, A., Varol, D., Breker, M., Strauss-Ayali, D., Viukov, S., Guilliams, M., Misharin, A., et al. (2013). Fate mapping reveals origins and dynamics of monocytes and tissue macrophages under homeostasis. Immunity *38*, 79–91.

Zigmond, E., and Jung, S. (2013). Intestinal macrophages: well educated exceptions from the rule. Trends Immunol. *34*, 162–168.